Süleyman Demirel Üniversitesi
Fen Bilimleri Enstitüsü Dergisi
Cilt 21, Sayı 3, 797-807, 2017

Süleyman Demirel University
Journal of Natural and Applied Sciences
Volume 21, Issue 3, 797-807, 2017

DOI: 10.19113/sdufbed.88484

Radon Concentration Measurements and Risk Assessments Around Uludağ Mountain (Bursa, Turkey)

Ayşegül KAHRAMAN*[1], Gizem AKKAYA[1], Gökay KAYNAK[1]

[1]Uludağ University, Faculty of Arts and Science, Physics Deparment, 16059, Bursa

(Alınış / Received: 03.05.2017, Kabul / Accepted: 26.07.2017, Online Yayınlanma / Published Online: 12.09.2017)

Keywords
Radon,
Groundwater,
Tap water,
Soil,
Dose

Abstract: The radon concentrations in the groundwater, tap water samples and soil gases of the residential areas and forested lands of Uludağ were measured to research on the dynamics of low-high radon levels over the various rocks types found in this area. Besides, the annual effective doses for groundwater and tap waters were calculated and compared with the recommended dose value by the World Health Organization (WHO) to evaluate the health risk of inhabitant. The radon concentrations in water samples for the wet and dry seasons were found in the ranges of 0.17 ± 0.09 - 195.64 ± 6.87 Bq l^{-1} (median value of 5.13 Bq l^{-1}) and 0.04 ± 0.01 - 199.24 ± 6.54 Bq l^{-1} (median value of 4.33 Bq l^{-1}), respectively. Elevated radon concentrations were measured in the waters draining through igneous rocks (granite and granodiorite), known as uranium-rich rocks. The average radon and thoron concentrations of soil gases were found to be in the ranges of 0.65 ± 0.01 – 199.66 ± 3.27 kBq m^{-3} and 4.36 ± 0.36 – 245.9 ± 7.26 kBq m^{-3}, respectively. The highest and lowest radon and thoron concentrations in soil gases were observed in the granitic area and in scree region, respectively.

Uludağ Çevresi Radon Konsantrasyon Ölçümleri ve Risk Değerlendirmeleri (Bursa, Türkiye)

Anahtar Kelimeler
Radon,
Yeraltusuyu,
Musluk suyu,
Toprak,
Doz

Özet: Uludağ'ın ormanlık arazileri ve yerleşim alanlarının toprak gazı, yeraltı ve musluk sularındaki radon konsantrasyonları, bu alandaki çeşitli kayaç tipleri boyunca düşük-yüksek radon seviye dinamiklerini araştırmak için ölçülmüştür. Ayrıca bu alanda yaşayan insanlar açısından sağlık riskini değerlendirmek amacıyla, musluk ve yer altı suları için yıllık etkin dozlar hesaplandı ve bu sonuçlar, Dünya Sağlık Örgütü (WHO) tarafından tavsiye edilen değerle kıyaslandı. Yağışlı ve yağışsız mevsimler için su örneklerindeki radon konsantrasyonları sırasıyla, 0.17 ± 0.09 Bq l^{-1}-195.64 ± 6.87 Bq l^{-1} (5.13 Bq l^{-1} medyan değeri) ve 0.04 ± 0.01 Bq l^{-1}-199.24 ± 6.54 Bq l^{-1} (4.33 Bq l^{-1} medyan değeri) aralıklarında bulundu. Yüksek radon konsantrasyonları, uranyumca zengin kayaçlar olarak bilinen volkanik kayaçlar (granit ve granitoyit) boyunca akan sularda ölçüldü. Toprak gazındaki ortalama radon ve toron konsantrasyonları sırasıyla 0.65 ± 0.01 – 199.66 ± 3.27 kBq m^{-3} ve 4.36 ± 0.36 – 245.9 ± 7.26 kBq m^{-3} aralıklarında bulundu. Toprak gazındaki en yüksek ve en düşük radon ve toron konsantrasyonları sırasıyla, granitik alanda ve yassı çakıl bölgede gözlemlendi.

1. Introduction

^{222}Rn, with a half-life of 3.82 days, is a radioactive, water-soluble noble gas continuously produced from the natural radioactive decay of radium in rocks and soil as part of the uranium decay chain. ^{222}Rn has no smell, colour or taste. Radon and its decay products are the most important contributors to inhalation exposure [1]. Darby et al. [2] reported that radon accounts for approximately 9% of all lung cancer deaths and 2% of total cancer deaths in Europe.

Most of the radon in indoor air comes from soil underneath the home. Radon in soil migrates to surface and concentrates enclosed spaces like building [3]. Dissolved radon in water also contributes to the radon concentration in the indoor air of dwellings, and this ratio depends on several

**Corresponding author: deepersea1981@gmail.com*

factors, such as the specific activity of radon in water used at homes and the amount of water consumed. The risk of excessive radon concentrations must be considered and necessary precautions must be taken to avoid the use of radon-rich sources or to apply effective treatment that reduces the radon content of these sources to reasonable levels [4]. The United States Environmental Protection Agency (US EPA) recommends that, in states or communities that choose not to develop a multimedia mitigation (MMM) program, action should be taken if the ^{222}Rn activity concentration of drinking water exceeds a maximum contaminant level (MCL) of 11.1 Bq l^{-1}. So, water systems already at or below 11.1 Bq l^{-1} standard would not be required to reduce their radon level. This value increases to an alternative maximum contaminant level (AMCL) of 148 Bq l^{-1} (4000 pCi l^{-1}) for states or communities that implement a multimedia mitigation (MMM) program [5]. The World Health Organization (WHO) reports that, if the radon activity concentration in drinking water for public water supplies exceeds 100 Bq l^{-1}, appropriate treatment should be applied to decrease the radon content to below this value [4].

Radon has much greater mobility than uranium and radium, which are present in all terrestrial materials, and it can escape relatively easily from rocks and soil through fractures and pore spaces. The radon concentration of groundwater is related to the geohydrological characteristics of the rock through which it flows. After radon is produced in underground rocks containing natural uranium, it is then released into the groundwater [4]. In other words, the rock type plays an important role in the radon concentration of groundwater [6-7]. Uranium and thorium concentrations generally increase with the SiO_2 content of rock during the differentiation, fractional crystallization, partial melting, etc. in final stage of the magmatic procedures [8]. These elements enhance in radiogenic accessory minerals such as allanite, monazit, zircon, apatite, sphene, thorite etc. that enhance in silica-saturated acidic magmatic rocks such as granite, rhyolite, syenite and pegmatite compared with intermediate, basic and ultrabasic rocks [8-10]. Therefore, such rocks cause elevated radiation levels. Besides, sedimentary rocks generally have lower levels of natural radionuclides than igneous rocks [1, 11]. Geologic fault zones also play an important role on the radon level. Numerous studies have shown that radon has higher level in the place close to the active fault zones since the fault lines provide the transportation of the radon gas towards the Earth's surface [12-14].

Uludağ mountain is a marked region to evaluate the radon from different points of view. The requirements of drinking water of villages and towns in Uludağ mountain as well as 20% of Bursa province have been supplied by springs in this region [15], and some spring waters of Uludağ mountain have been commercially used. For these reasons, determination of the radon concentrations of the springs and tap waters at this region is quite important for evaluation of the radiologic risk. Especially, high radon concentrations in some areas could be expected due to their geological structures composed of igneous rocks. Another reason of this expectation is that most of the groundwater circulation in the Uludağ region occurs in fractures and comes out in the form of spring [16]. However, relationship between the geology and radon concentration in the region could be exhibited by means of the radon concentration results that will be obtained from soil gases and springs. In the light of the motivations stated above, the aims of the present study is: i) to measure radon concentration in groundwater (in spring form) related with aquifers in contact with different rocks, ii) to determine the health risk for the inhabitant by using the radon concentration results of tap water and groundwater, iii) to measure radon -thoron concentrations of soil gases of the region and to assess the results from geological point of view. With the best of our knowledge, the radon and thoron concentrations of Uludağ mountain have been extensively studied for the first time with this study.

2. Material and Method

Uludağ, formerly known as Olympus Misius, is located between the latitudes of 39° 45' - 40° 10' N and the longitudes of 28° 58' - 29° 38' E. It is the highest mountain (2543 m) in the Marmara region of Turkey and one of the most popular ski resorts in Turkey. Up to now, the most comprehensive geology map of Uludağ mountain has been presented by Okay et al. [17], but, this figure has not included the eastern part of the study area. Therefore, geologic table of whole of the study area was prepared by means of the other studies in the literature and the references were given on this table (Table 1).

The 45 water samples (20 tap water and 25 groundwater samples) were collected from 37 different locations on Uludağ mountain during the spring (wet) and summer (dry) seasons of 2012, their radon concentrations were measured. Collected groundwaters are in the spring form. Besides, spring waters are stored in the water tanks of the villages and are distributed to the houses as tap water. Soil gases measurements were performed at 24 different locations. The sampling locations are demonstrated on the map, roughly prepared using Surfer 8.0 and Google Earth (ver. 7.0.2) (Figure 1).

Water samples were taken from their sources and directly placed into the 500 ml polyethylene bottles. The bottles were completely filled and immediately closed tightly in order to prevent bubbles and radon escape. Afterwards, the samples were transported to the Environmental Physics Laboratory of Uludağ University for measurement. Soil gas measurements were performed at the sampling areas.

Table 1. Water types of the samples and the geological properties of the studied regions

No.	Location	Water type	Geological Setting
1	Yiğitali	GW	Conglomeras, coloured gre and marls, limestones, tuff [17, 18]
2	Summit road-1	GW	Glaucophane-greenschist, gneiss, amphibolite [17, 19]
3	Summit road-2	GW	
4	Hüseyinalan	TW	Glaucophane-greenschist, marbles on the schists [19]
5	Summit road-3	GW	
6	Hüseyinalan road	GW	
7	Kirazlı	TW	Diorite from spilitic rock series, marbles on the schists Two-mica granodiorite (east of the area) [15, 19]
8	Süleymaniye	GW	Gneiss, amphibolite Two-mica granodiorite (east of the area) [15, 19]
9	Kirazlıyayla	TW	Two-mica Central Uludağ Granite [17],Two-mica granodiorite [15]
10	Sarıalan	TW	
11	Summit road-4	GW	
12	Summit road-5	GW	
13	Oteller-1	GW	
14	Oteller-2	GW	
15	Soğukpınar	TW	Peridotite, gabbro, diabase [17, 20]
16	Cumalıkızık	TW	Scree [17]
17	Hamamlıkızık	GW	Talus [21]
18	Derekızık	TW	Scree Marble, gneiss and amphibolite (south of the areas) [17]
19	Saitabat-1	TW	
20	Saitabat-2	GW	
21	Burhaniye	TW	
22	Alaçam	TW	Metabasite, marble, phyllite [17, 20]
23	Şevketiye	GW	
24	Güneybayırı	GW	
25	Çaybaşı	GW	metabasite, marble, phyllite, alluvial deposits, silty-sandy gravel with rounded granite, and amphibolites boulders in the region [16, 17]
26	Güneybudaklar-1	GW	Peridotite, gabbro, diabase, sandstone, shale, conglomerate, tuff, granodiorite [17]
27	Güneybudaklar-2	GW	
28	Dağdibi	TW	Sandstone, shale, conglomerate, tuff Gneiss, amphibolite (north of the area) [17]
29	Baraklı-1	TW	Peridotite, gabbro, diabase Blueschist mica schist, marble Sandstone, shale, conglomerate, tuff Gneiss, amphibolite (north of the area) [17]
30	Baraklı-2	GW	
31	Kıran	TW	Classical facies of Neogene [19]
32	Fevziye	TW	-
33	Lütfiye	TW	-
34	Boğazova-1	TW	Boğazova granodiorite [22]
35	Boğazova-2	GW	
36	Boğazova road	GW	-
37	İclaliye	TW	Sandstone, claystone [23]
38	Saadet-1	TW	Granite, quartzite, diorite [24]
39	Saadet-2	GW	
40	Hamidiye	TW	Sandstone, claystone [23]
41	Tahtaköprü-1	TW	Clay, conglomera, gravel, Granite (nearly 2-3 km south of Tahtaköprü) [25-28]
42	Tahtaköprü-2	GW	
43	Mesruriye-1	GW	Granite, quartzite, diorite [24]
44	Mesruriye-2	GW	
45	Oylat	GW	Granite, quartzite, diorite, marble, crystallized limestone [29]

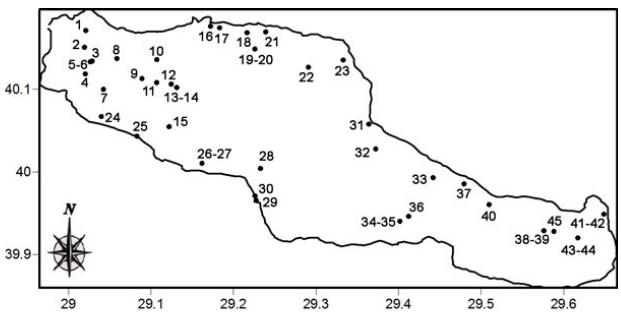

Figure 1. Study area

The radon concentrations in the water samples were measured using a professional radon monitor AlphaGUARD PQ 2000PRO (GENITRON, Germany). The AlphaGUARD uses a cylindrical ionization chamber (an active volume of 0.56 L). Radon concentrations in soil gas, water and air can be measured with this system. This system has also been designed to measure the thoron in soil gas. The system has a fast response to concentration gradients and its detection efficiency is high. AlphaGUARD with an AquaKIT set-up can directly detect radon and indirectly detect radium in water samples.

Detailed experimental processes and methods for waters and soil gas were given in our previous study [30].

2.1. Dose calculations

Radon exposure from waters may occur either from ingestion or from inhalation of radon released from water [4]. Radon and its decay products deposit along the walls of the various airways of the bronchial tree by inhalation. This is the most important pathway for radiation exposure in the lungs. Alpha particles provide the main contribution to exposure compared to gamma radiation and beta particles. Alpha particle irradiation of the secretory and basal cells of the upper airway is responsible for the lung cancer risk in miner [1]. Water goes to the stomach with its consumption and before the leaving; some of the dissolved radon can diffuse through the stomach wall. Cells interact with radiation emitted from radon and its decay products, which can pass through the wall and absorbed in blood. Therefore, radiation dose is transported to other parts of the body [31]. It is known that radon ingestion causes stomach cancer. For these reasons, both inhalation and ingestion parameters should be considered when evaluating radon dose limits. Using the following formula, the annual effective doses were calculated with different consumption rates:

$$D_{ing} = C \times V \times F \quad (1)$$

where C is the radionuclide activity concentration in water (Bq l^{-1}) and F is the effective dose equivalent conversion factor for ingestion. The recommended F value is 3.5 nSv Bq^{-1} without any distinction between age groups by NRC [32-33]. V is the volume of water ingested annually, which is assumed to be 60 l y^{-1} (weighted estimate of consumption) by UNSCEAR [1] and 730 l y^{-1} by WHO [4]. However, consumers receive an additional dose from radon decay products, such as ^{210}Po.

The annual effective dose rates for inhalation of a radon source from water usage were calculated using the following equation:

$$D_{inh} = C \times TF \times F \times F_{inh} \times T \quad (2)$$

where C is the radionuclide activity concentration in water (Bq l^{-1}), TF is the air water concentration rate (10^{-4}), F is the indoor equilibrium factor between radon and its progenies (0.4), F_{inh} is the dose conversion factor for radon exposure (9 nSv (Bq h $m^{-3})^{-1}$), and T is the exposure time (0.8×24 h×365≈7000 h y^{-1}) [1]. Some of the water samples are used only for drinking, but, D_{inh} values were calculated for all samples to give a rough estimation.

3. Results

The results of radon concentration measurements in tap water and groundwater (in the form of spring) samples are presented in Table 2. The radon concentration levels varied from 0.17 ± 0.09 to 195.64 ± 6.87 Bq l^{-1}, with an average value of 24.81 ± 7.09 Bq l^{-1} in the wet season, and from 0.04 ± 0.01 to 199.24 ± 6.54 Bq l^{-1}, with an average value of 26.00 ± 7.16 Bq l^{-1} in the dry season. The average radon concentrations of water samples measured in both seasons are 25.61 ± 7.48 Bq l^{-1} for the wet season and 21.95 ± 7.92 Bq l^{-1} for the dry season. The radon and thoron concentrations of soil gases are given in Table 2. The values were ranged from 0.65 ± 0.01 to 199.66 ± 3.27 kBq m^{-3} for ^{222}Rn and from 4.36 ± 0.36 to 245.95 ± 7.26 kBq m^{-3} for ^{220}Rn.

Detailed descriptive statistics obtained from the water samples and soil gases are given in Table 3. A total of 30% of the tap water and 48% of the groundwater samples were measured more than the MCL (11.1 Bq l^{-1}) value recommended by US EPA for public drinking water supplies. In addition, two samples exceeded the AMCL (148 Bq l^{-1}) of US EPA. The values for the wet and dry seasons followed a log-normal distribution for radon concentrations in water samples. Besides, soil gases results can be fitted to log-normal distribution.

According to the average values, a statistically significant difference in the radon concentrations of water samples was not found between the wet and dry seasons. Pearson's correlation coefficient was calculated between the radon activity concentrations of the waters (both wet and dry seasons) and soil gases using a statistical package program (SPSS ver. 20.0) and positive correlation values, r = 0.317, p=0.141 for wet season and r = 0,312, p = 0,148 for dry season, were obtained. These values show that there is no statistically significant correlation between the radon concentrations of waters and soil gases.

The highest radon concentration for water samples was found to be 199.24 ± 6.54 Bq l^{-1} in the dry season (sample-11). This cold groundwater source was underlain by granitic bedrock [34]. The high uranium content of this igneous rock causes the elevated radon concentrations in the groundwaters. The highest radon and thoron levels in soil gases were measured in one of the granitic areas of the Uludağ mountain (location-38) as 199.66 ± 3.27 kBq m^{-3} and 245.95 ± 7.26 kBq m^{-3}, respectively. On the basis of the results, contour maps of radon and thoron concentrations were shown in Figure 2.

Table 2. Radon concentrations in soil gases and water samples (Hyphens (-) show that no measurements have been made)

No.	Location	Water type	Radon (Bq l^{-1}) (Spring)	Radon (Bq l^{-1}) (Summer)	^{222}Rn in soil (kBq m^{-3})	^{220}Rn in soil (kBq m^{-3})
1	Yiğitali	GW	3.48 ± 0.12	2.28 ± 0.37	-	-
2	Summit road-1	GW	1.20 ± 0.19	2.46 ± 0.41	-	-
3	Summit road-2	GW	4.91 ± 0.41	9.25 ± 0.12	-	-
4	Hüseyinalan	TW	0.17 ± 0.09	0.04 ± 0.01	-	-
5	Summit road-3	GW	0.26 ± 0.10	0.28 ± 0.08	-	-
6	Hüseyinalan road	GW	1.17 ± 0.17	2.56 ± 0.30	-	-
7	Kirazlı	TW	27.55 ± 0.55	11.20 ± 0.64	-	-
8	Süleymaniye	GW	43.56 ± 1.02	24.35 ± 0.42	-	-
9	Kirazlıyayla	TW	96.57 ± 0.12	63.89 ± 7.87	22.69 ± 0.54	54.46 ± 3.30
10	Sarıalan	TW	116.51 ± 1.59	31.51 ± 5.99	46.16 ± 0.98	65.99 ± 1.92
11	Summit road-4	GW	195.64 ± 6.87	199.24 ± 6.54	76.27 ± 1.63	95.57 ± 3.09
12	Summit road-5	GW	85.43 ± 14.8	184.19 ± 2.38	-	-
13	Oteller-1	GW	92.59 ± 2.63	70.13 ± 2.28	73.08 ± 3.20	98.08 ± 3.97
14	Oteller-2	GW	-	147.20 ± 3.02	-	-
15	Soğukpınar	TW	3.89 ± 3.20	0.99 ± 0.01	10.09 ± 0.46	34.05 ± 2.20
16	Cumalıkızık	TW	4.87 ± 0.11	0.69 ± 0.01	0.65 ± 0.01	5.97 ± 0.48
17	Hamamlıkızık	GW	6.81 ± 0.06	2.11 ± 0.60	12.44 ± 0.47	25.65 ± 0.81
18	Derekızık	TW	9.18 ± 0.11	7.37 ± 0.25	6.10 ± 0.19	11.43 ± 0.40
19	Saitabat-1	TW	1.48 ± 0.15	1.03 ± 0.24	-	-
20	Saitabat-2	GW	-	0.48 ± 0.14	-	-
21	Burhaniye	TW	2.14 ± 0.06	1.36 ±0.10	1.15 ± 0.11	4.36 ± 0.36
22	Alaçam	TW	4.35 ± 0.23	2.75 ± 0.21	6.36 ± 0.17	8.25 ± 0.25
23	Şevketiye	GW	1.35 ± 0.13	0.60 ± 0.22	15.34 ± 0.45	32.92 ± 1.95
24	Güneybayırı	GW	2.68 ± 0.19	0.38 ± 0.13	9.89 ± 0.36	23.88 ± 1.08
25	Çaybaşı	GW	54.17 ± 1.20	26.78 ± 1.86	22.94 ± 0.60	72.92 ± 7.07
26	Güneybudaklar-1	GW	20.16 ± 0.44	22.24 ± 1.01	23.87 ± 0.50	23.44 ± 0.76
27	Güneybudaklar-2	GW	-	82.63 ± 3.11	-	-
28	Dağdibi	TW	31.38 ± 0.92	18.44 ± 2.28	43.81 ± 1.01	73.27 ± 3.86
29	Baraklı-1	TW	20.92 ± 0.70	21.20 ± 1.21	18.49 ± 0.72	42.04 ± 1.45
30	Baraklı-2	GW	-	48.15± 2.07	-	-
31	Kıran	TW	2.29 ± 0.45	-	-	-
32	Fevziye	TW	1.31 ± 0.17	3.15 ± 0.07	13.47 ± 0.62	19.06 ± 0.61
33	Lütfiye	TW	1.62 ± 0.69	3.10 ± 0.57	15.53 ± 0.59	34.82 ± 1.59
34	Boğazova-1	TW	-	23.37 ± 1.08	26.20 ± 0.71	155.65 ± 7.09
35	Boğazova-2	GW	-	58.96 ± 1.75	-	-
36	Boğazova road	GW	1.96 ± 0.02	7.40 ± 0.50	-	-
37	İclaliye	TW	6.24 ± 1.78	4.07 ± 1.55	7.56 ± 0.45	158.38 ± 6.44
38	Saadet-1	TW	6.39 ± 0.48	4.51 ± 0.48	199.66 ± 3.27	245.95 ± 7.26
39	Saadet-2	GW	-	4.13 ± 0.43	-	-
40	Hamidiye	TW	5.35 ± 0.23	0.55 ± 0.16	10.40 ± 0.45	111.76 ± 5.93
41	Tahtaköprü-1	TW	1.95 ± 0.01	4.15 ± 0.35	7.32 ± 0.79	51.11 ± 3.86
42	Tahtaköprü-2	GW	20.1 ± 0.47	-	-	-
43	Mesruriye-1	GW	13.45 ± 0.40	12.08 ± 0.77	12.95 ± 0.74	69.12 ± 5.57
44	Mesruriye-2	GW	-	4.33 ± 0.39	-	-
45	Oylat	GW	-	2.34 ± 0.25	-	-
	Average values		24.81 ± 7.09	26.00 ± 7.16	28.43 ± 8.49	63.26 ± 11.89

Table 3. Statistical results for the radon and thoron concentrations (Bq l^{-1} for water and kBq m^{-3} for soil)

Statistics	Wet	Dry	Wet*	Dry*	Soil (^{222}Rn)	Soil (^{220}Rn)
Median	5.13	4.33	4.11	5.13	14.41	46.58
Arithm. mean ± S.E.	24.81 ± 7.09	26.00 ± 7.16	21.95 ± 7.92	25.61 ± 7.48	28.43 ± 8.49	63.26 ± 11.89
S.D.	42.52	46.95	46.19	43.59	41.59	58.25
Geometric mean	6.81	5.99	4.82	6.82	14.77	40.88
Range	0.17 – 195.64	0.04 – 199.24	0.04 – 199.24	0.17 – 195.64	0.65 – 199.66	4.36 – 245.95
Skewness	2.540	2.645	3.223	2.454	3.369	1.654
Kurtosis	6.999	6.766	10.225	6.460	13.011	3.086
Frequency distribution	Log-normal (p<0.001)	Log-normal (p<0.001)	Log-normal (p<0.001)	Log-normal (p<0.001)	Log-normal (p<0.001)	Log-normal (p<0.001)

* The radon concentrations of some water samples were measured at both seasons. The statistical results given with star (*) were calculated solely based on these examples.

Potential annual dose rates for inhalation and ingestion due to the consumption of water have been estimated using radon activity concentrations and water consumption rates of 1 l d^{-1} and 2 l d^{-1}; the results are presented in Table 4. The WHO [4] reported the recommended reference dose level as 0.1 mSv y^{-1}, taken from the total possible radioactive contamination of annual drinking water consumption. Some of the water samples, demonstrated in bold style, exceeded 0.1 mSv y^{-1} (Table 4).

4. Discussion and Conclusion

The region was divided into five different parts for the interpretation of the radon and thoron concentrations. The areas (from sample-1 to 6) in the first part are on the summit road. All of the radon concentrations of the water samples have low values. Therefore, calculated effective doses for ingestion and inhalation have not important levels from the health risk point of view.

The areas (from the sample-7 to 14) in the second part are also on the summit road. The results obtained from these areas demonstrated that radon concentrations in the tap water and groundwater samples begin to rise towards the summit region. This finding is consistent with the volcanic origin of aquifer rocks in this region. These rocks form the catchment area that feeds water to the springs. Besides, the radon and thoron concentrations in the soil gases of these areas are relatively in high levels. In our previous study [35], the ^{226}Ra and ^{232}Th activity concentrations of the Oteller region (near location-13) were reported to be 61 ± 3 Bq kg^{-1} and 33 ± 1 Bq kg^{-1}, respectively. Not only the rock type plays an important role in the radon concentrations but also the mineral content of the rocks is important from this point of view. Yurdagül [15] reported that the upper Oligocene granodioritic rocks of the Uludağ are represented by a medium to high potassic, calc-alkaline, peraluminous and dominantly acidic character. The accessory minerals are zircon, apatite, allanite, sphene, epidote, and monazite in the granodiorite. The zircon and apatite minerals of acidic crystalline rocks are important to evaluate the natural radionuclide levels. Zircon and apatite are known as uranium-rich minerals, and uranium and thorium are present within their crystal structures [36-37]. In addition, many cracks and fractures were observed in Uludağ granodiorite and marbles [15]. Thus, radon can move easily through the cracks and fractures in these rocks. The seasonal variation of the radon concentrations in waters of this part was observed as more distinctive in the two samples (sample-10 and 12). The reason of a significant reduction in radon content of the water (sample-10) in dry season may be the rinse out effect [38]. The increase in the radon concentration of sample-12 in the dry season can be attributed to the rainfall amount. During the wet season, snow-melt and rain water can infiltrate into the groundwater system and dilute the radon concentration. Another possible explanation is that if this spring is fed by deep aquifers, the rainfall contribution to its flow can be delayed [39-40]. Due to the high radon contents in the waters, calculated effective doses for ingestion and inhalation in the both seasons have high levels. The radon concentration results of soil gases for sample 11 and 13 demonstrate that these areas have high risk (> 50 kBq m^{-3}) from the radiological point of view. The radon risk for the other areas, sample 9 and 10, is at the normal level (10 – 50 kBq m^{-3}) [40].

The third part of the region contains the samples from 15 to 24. Both waters and soil gases results show the quite low values compared the other parts of the region. The most interesting result in this part was obtained from the Soğukpınar (sample-15). Although igneous rocks (peridotite, gabbro, and diabase) are observed in this village, radon and thoron concentrations are lower than expected. Therefore, investigation of the structures of the rocks is important to evaluate the relationship between the geology and radon-thoron contents. Peridotites are ultramafic igneous rocks and their silica contents are low compared to other igneous rocks such as granite. Besides, they contain very little quartz and feldspar. Gabbro shows the similar properties with peridotites. It has low silica content and no quartz, alkali feldspar. Chemically and mineralogically, diabase resembles the volcanic basalt or plutonic gabbro. The reason of the low radon and thoron values may be attributed to low silica content of rocks [8].

On the other side, the low radon concentrations in soil gases were also measured in the areas with metabasite, marble, and phyllite. Metabasites are known as metamorphosed basic igneous rocks. It was reported that the radium content of basic igneous rocks is quite low compared to the acidic igneous rocks such as granite and these regions are defined as low radon risk areas [40]. Marble is a rock resulting from metamorphism of sedimentary carbonate rocks, most commonly limestone or dolomite rock. Phyllite is a fined grained metamorphic rock created from slate that is a low grade metamorphic rock generally formed by the metamorphosis of mudstone/shale (sedimentary origin), or sometimes basalt, under relatively low pressure and temperature conditions. Low radon concentrations are generally expected in sedimentary rocks [1, 9, 11, 40]. Due to the low radon contents in the waters, calculated effective doses for ingestion and inhalation in the both seasons have low levels. This part can be defined as low (< 10 kBq m^{-3}) and normal risk areas (10 – 50 kBq m^{-3}) [40].

The fourth part of the region contains the samples from 25 to 30. The radon concentrations in waters exceed the US EPA MCL (11.1 Bq l^{-1}). The reason of the relatively higher radon contents compared to third part of the region may be explained by the evaluating the hydrogeology of location-25 which was investigated in detail by [16]. There are deep groundwater flow and shallow aquifer at this sampling location. Shallow groundwater generally flows through the metabasites (Karakaya formation), while deep groundwater flow emanates from bedrock composed of fractured granite, gneiss and serpentine rocks. Therefore, relatively higher radon levels can be observed in this area.

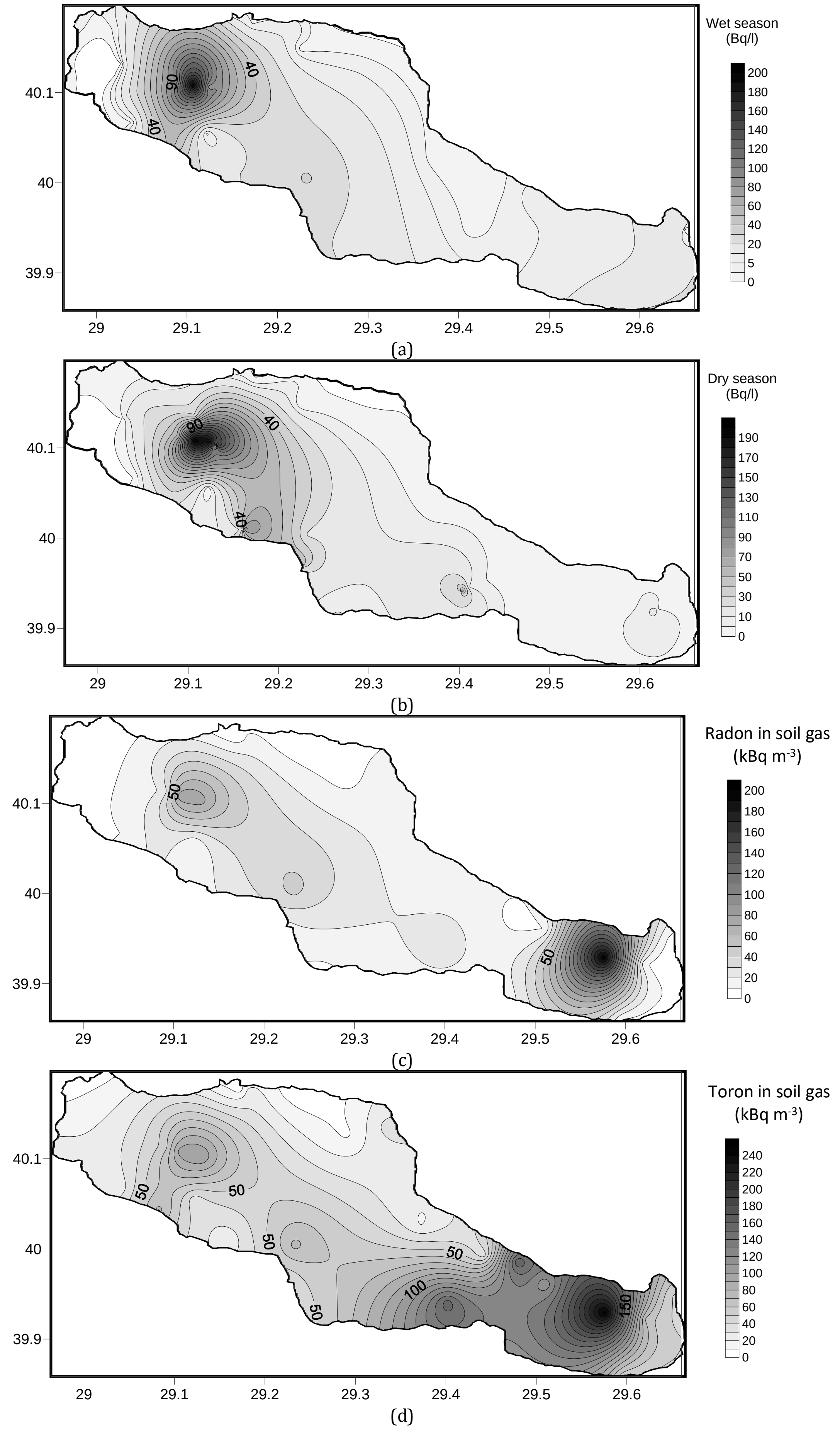

Figure 2. (a) Contour map of radon concentration results of waters in wet season, (b) Contour map of radon concentration results of waters in dry season, (c) Contour map of radon concentration results of soil gases, (d) Contour map of thoron concentration results of soil gases

Table 4. Calculated effective doses for ingestion and inhalation for wet and dry seansons

No.	Water type	Ingestion (Wet) (mSv/y) 1 l d^{-1}	Ingestion (Wet) (mSv/y) 2 l d^{-1}	Inhalation (Wet) (mSv/y)	Ingestion (Dry) (mSv/y) 1 l d^{-1}	Ingestion (Dry) (mSv/y) 2 l d^{-1}	Inhalation (Dry) (mSv/y)
1	GW	0.0044	0.0089	0.0088	0.0029	0.0058	0.0057
2	GW	0.0015	0.0031	0.0030	0.0031	0.0063	0.0062
3	GW	0.0063	0.0125	0.0124	0.0118	0.0236	0.0233
4	TW	0.0002	0.0004	0.0004	0.0001	0.0001	0.0001
5	GW	0.0003	0.0007	0.0007	0.0004	0.0007	0.0007
6	GW	0.0015	0.0030	0.0030	0.0033	0.0065	0.0064
7	TW	0.0352	0.0704	0.0694	0.0143	0.0286	0.0282
8	GW	0.0556	**0.1113**	0.1098	0.0311	0.0622	0.0614
9	TW	**0.1234**	**0.2467**	0.2434	0.0816	**0.1632**	0.1610
10	TW	**0.1488**	**0.2977**	0.2936	0.0403	0.0805	0.0794
11	GW	**0.2499**	**0.4999**	0.4930	**0.2545**	**0.5091**	0.5021
12	GW	**0.1091**	**0.2183**	0.2153	**0.2353**	**0.4706**	0.4642
13	GW	**0.1183**	**0.2366**	0.2333	0.0896	**0.1792**	0.1767
14	GW	-	-	-	**0.1880**	**0.3761**	0.3709
15	TW	0.0050	0.0099	0.0098	0.0013	0.0025	0.0025
16	TW	0.0062	0.0124	0.0123	0.0009	0.0018	0.0017
17	GW	0.0087	0.0174	0.0172	0.0027	0.0054	0.0053
18	TW	0.0117	0.0235	0.0231	0.0094	0.0188	0.0186
19	TW	0.0019	0.0038	0.0037	0.0013	0.0026	0.0026
20	GW	-	-	-	0.0006	0.0012	0.0012
21	TW	0.0027	0.0055	0.0054	0.0017	0.0035	0.0034
22	TW	0.0056	0.0111	0.0110	0.0035	0.0070	0.0069
23	GW	0.0017	0.0034	0.0034	0.0008	0.0015	0.0015
24	GW	0.0034	0.0068	0.0068	0.0005	0.0010	0.0010
25	GW	0.0692	**0.1384**	0.1365	0.0342	0.0684	0.0675
26	GW	0.0258	0.0515	0.0508	0.0284	0.0568	0.0560
27	GW	-	-	-	**0.1056**	**0.2111**	0.2082
28	TW	0.0401	0.0802	0.0791	0.0236	0.0471	0.0465
29	TW	0.0267	0.0535	0.0527	0.0271	0.0542	0.0534
30	GW	-	-	-	0.0615	**0.1230**	0.1213
31	TW	0.0029	0.0059	0.0058	-	-	-
32	TW	0.0017	0.0033	0.0033	0.0040	0.0080	0.0079
33	TW	0.0021	0.0041	0.0041	0.0040	0.0079	0.0078
34	TW	-	-	-	0.0299	0.0597	0.0589
35	GW	-	-	-	0.0753	**0.1506**	0.1486
36	GW	0.0025	0.0050	0.0049	0.0095	0.0189	0.0187
37	TW	0.0080	0.0159	0.0157	0.0052	0.0104	0.0103
38	TW	0.0082	0.0163	0.0161	0.0058	0.0115	0.0114
39	GW	-	-	-	0.0053	0.0106	0.0104
40	TW	0.0068	0.0137	0.0135	0.0007	0.0014	0.0014
41	TW	0.0025	0.0050	0.0049	0.0053	0.0106	0.0105
42	GW	0.0257	0.0514	0.0507	-	-	-
43	GW	0.0172	0.0344	0.0339	0.0154	0.0309	0.0304
44	GW	-	-	-	0.0055	0.0111	0.0109
45	GW	-	-	-	0.0030	0.0060	0.0059

The bedrock of the other water samples of this part may have similar properties with sample-25. Although sample 26 and 27 were collected from same area, the measured radon values in waters are quite different from each other. This finding shows that catchment areas are not composed of the same aquifer rocks. The high radon content of the sample 27 may be due to the granodiorite (igneous rock) observed in this village. The radon concentrations of soil gases show that this part can be defined as normal risk area (10 – 50 kBq m^{-3}). Metabasite, marble, phyllite peridotite, gabbro, diabase, shale from the observed rocks in this part may have the low radium content as discussed above. Sandstone and conglomerate are the sedimentary rocks. Tuff is also a sedimentary rock formed by the accumulation of volcanic ash plus. Schist is medium grade metamorphic rock, formed by the metamorphosis of mudstone (sedimentary rock)/ shale, or some types of igneous rock [16-17].

The last part of the region contains the samples from 31 to 45. The most interesting results for this part were obtained from the location-38. The quite low radon concentration in water was observed despite the highest radon and thoron contents in soil gas were observed in this village. The reason of the high radon and thoron contents in soil gases may be the granite rocks. The low radon content in waters (samples 38 – 39) may be a result of the hydrogeology of this location. The hydrogeology of the locations - 38, 39, 43, 44, 45 was studied in detail by Pasvanoglu [24]. According to this study, primary aquifers for thermal and cold waters are marbles in these locations. In addition, limestones (sedimentary rock) act as an aquifer. The sedimentary-rock aquifers may provide the low radon contents in waters. Another important result for soil gas was obtained from location-40 due to the low radon and high thoron. Lithology information is not enough to evaluate this result due to the fact that the radon and thoron concentrations are affected from several factors such and porosity, moisture. The highest radon concentrations in the waters of this part were measured in locations 34 – 35, where the main rock type is granodiorite, igneous rock. The major and accessory minerals of granodiorite were taken from the [22]. According to this study, the major minerals are quartz, plagioclase, orthoclase, hornblende, and biotite, and the accessory minerals are sphene, zircon, apatite, rutile, and opaque. Taking the rock type and mineral content (zircon and apatite) into account, it is an expected result as discussed above. Except this location, calculated effective doses for ingestion and inhalation in the both seasons generally have low levels in this part.

Prior to this study, there was no recorded data for the radon contents in the tap waters, groundwaters and soil gases of this region. The elevated radon concentrations were measured in waters draining through igneous rocks with high silica content. However, the lower radon values in the waters were observed in the igneous-rock with low silica content and sedimentary-rock aquifers. Despite the average radon concentrations in the both seasons are in the similar levels, the seasonal variations are observed in some areas. Elevated radon and thoron concentrations in soil gases were observed in the areas with igneous rocks while lower values were measured in the areas with sedimentary rocks. It is not found a statistically significant difference between the radon concentrations of waters and soil gases.

A total of 31% of the waters in wet season and 40% of the waters in dry season were measured more than the MCL (11.1 Bq l^{-1}) value recommended by US EPA for public drinking water supplies. A total of 14% of the waters in wet season and 16% of the waters in dry season exceed the reference dose level as 0.1 mSv y^{-1}. According to radon concentrations measurements of soil gases, 29%, 58%, and %12.5 of the locations can be classified as low, normal and high risk areas, respectively.

References

[1] United Nations Scientific Committee on the Effects of Atomic Radiation (UNSCEAR), 2000. Report to the General Assembly with Annexes. New York: United Nations Publication.

[2] Darby S., Hill D., Auvinen A., Barros-Dios J.M., Baysson H., Bochicchio F., Deo H., Falk R., Forastiere F., Hakama M., Heid I., Kreienbrock L., Kreuzer M., Lagarde F., Makelainen I, Muirhead C., Oberaigner W., Pershagen G., Ruano-Ravina A., Ruosteenoja E., Rosario A.S., Tirmarche M., Tomasek L., Whitley E., Wichmann H.E., Doll R. 2005. Radon in Homes and Risk of Lung Cancer: Collaborative Analysis of Individual Data from 13 European Case-Control Studies. British Medical Journal, 330(7485), 223-226.

[3] United Nations Scientific Committee on the Effects of Atomic Radiation (UNSCEAR), 2008. Effects of ionizing radiation. In: Annex E, Sources-to-Effects Assessment for Radon in Homes and Workplaces. New York: United Nations Publication.

[4] World Health Organization (WHO), 2008. Guidelines for Drinking-water Quality-Recommendations. Switzerland: WHO Press.

[5] US Environmental Protection Agency (US EPA), 2012. Report to Congress: Radon in Drinking Water Regulations. US EPA 815-R-12-002.

[6] Choubey, V.M., Ramola, R.C. 1997. Correlation between Geology and Radon Levels in Groundwater, Soil and Indoor Air in Bhilangana Valley, Garhwal Himalaya, India. Environmental Geology, 32(4), 258-262.

[7] Voronov, A.N. 2004. Radon-rich Waters in Russia. Environmental Geology, 46(5), 630-634.

[8] Örgün, Y., Altınsoy, N., Gültekin, A.H., Karahan, G., Çelebi, N. 2005. Natural Radioactivity Levels in Granitic Plutons and Groundwaters in Southeast Part of Eskisehir, Turkey. Applied Radiation and Isotopes, 63(2), 267-275.

[9] Ramola, R.C., Choubey, V.M., Prasad, Y., Prasad, G., Bartuya, S.K. 2006. Variation in Radon Concentration and Terrestrial Gamma Radiation Dose Rates in Relation to the Lithology in Southern Part of Kumaon Himalaya, India. Radiation Measurements, 41(6), 714-720.

[10] Orgun, Y., Altinsoy, N., Sahin, S.Y., Gungor, Y., Gultekin, A.H., Karahan, G., Karacik, Z. 2007. Natural and Anthropogenic Radionuclides in Rocks and Beach Sands from Ezine Region (Canakkale), Western Anatolia, Turkey. Applied Radiation and Isotopes, 65(6), 739-747.

[11] Marocchi, M., Righi, S., Bargossi, G.M., Gasporotto, G. 2011. Natural Radionuclides Content and Radiological Hazard of Commercial Ornamental Stones: An Integrated Radiometric and Mineralogical-Petrographic Study. Radiation Measurements, 46(5), 538-545.

[12] Zarroca, M., Linares, R., Bach, J., Roque, C., Moreno, V., Font, L., Baixeras, C. 2012. Integrated Geophysics and Soil Gas Profiles as a Tool to

Characterize Active Faults: the Amer Fault Example (Pyrenees, NE Spain). Environmental Earth Sciences, 67(3), 889-910.

[13] Seminsky, K.Z., Demberel, S. 2013. The First Estimations of Soil-Radon Activity near Faults in Central Mongolia. Radiation Measurements, 49, 19-34.

[14] Tarakçı, M., Harmanşah, C., Saç, M.M., İçhedef, M. 2014. Investigation of the Relationships between Seismic Activities and Radon Level in Western Turkey. Applied Radiation and Isotopes, 83, 12-17.

[15] Yurdagül, A. 2004. Uludağ Granitoyidinin Litojeokimyasal İncelenmesi. İstanbul Üniversitesi, Fen Bilimleri Enstitüsü, Yüksek Lisans Tezi, 139s, İstanbul.

[16] Boiero, D., Godio, A., Naldi, M., Yigit, E. 2010. Geophysical Investigation of a Mineral Groundwater Resource in Turkey. Hydrogeology Journal, 18(5), 1219-1233.

[17] Okay, A.I., Satir, M., Zattin, M., Cavazza, W., Topuz, G. 2008. An Oligocene Ductile Strike-Slip Shear zone: The Uludag Massif, Northwest Turkey – Implications for the Westward Translation of Anatolia. Geological Society of Amerika Bulletin, 120(7-8), 893-911.

[18] Ketin, İ. 1947. About the Tectonic of Uludağ Massif. Türkiye Jeoloji Kurumu Bülteni, 1, 60-88.

[19] Kaaden, G.v.d. 1959. Güneybatı Türkiye'de Peridotite Kitleleri İçinde Zuhur Eden Kromitlerin Kompozisyonu ile Tektonik-Magmatik Vaziyetleri Arasındaki Münasebet Hakkında. Maden Tetkik ve Arama Enstitüsü, 52, 15-34.

[20] Okay, A.I. 2009. Bursa Arazi Gezisi. https://web.itu.edu.tr/~okay/dersler/bursagezi.pdf (Erişim Tarihi: 27.04.2017).

[21] Akyol, N., Akinci, A., Eyidogan, H. 2002. Site Amplification of S-waves in Bursa City and Its Vicinity, Northwestern Turkey: Comparison of Different Approaches. Soil Dynamics and Earthquake Engineering, 22(7), 579-587.

[22] Sendir, H., Sarıiz, K. 2009. The Geochemical Characteristics of the Bogazova Granitoid (KUTAHYA). Anadolu University Journal of Science and Technology, 10(2), 431-445.

[23] Cengiz, İ., Genç, Y. 2003. Domaniç (Kütahya) Bakır-Molibden Cevherleşmesinin Jeolojisi ve Alterasyon Özellikleri. Jeoloji Mühendisliği Dergisi, 27(2), 47-75.

[24] Pasvanoglu, S. 2011. Hydrogeochemical and Isotopic Investigation of the Bursa-Oylat Thermal Waters, Turkey. Environmental Earth Sciences, 64(4), 1157-1167.

[25] Maden Tetkik ve Arama Genel Müdürlüğü (MTA), 1979. MTA Raporları: Bursa-İnegöl-Tahtaköptü-Demir Tepe Dolayı Vollastonit Aramaları Ara Raporu. https://eticaret.mta.gov.tr/index.php?route=product/product&product_id=6903 (Erişim Tarihi: 20.06.2017).

[26] T.C. İnegöl Belediyesi, 2016. İnegöl-Yenice (Bursa) Islah Organize Sanayi Bölgesi Amaçlı 1/1.000 Ölçekli Uygulama İmar Planı Revizyonu Açıklama Raporu. http://www.inegol.bel.tr/media/documents/4518_1480402283.pdf (Erişim Tarihi: 20.06.2017).

[27] Demange, M., Berson, F., Fonteilles, M., Pascal, M.-L., Öngen, S., F., M.-C., 1998. Wollastonite-garnet Skarns of Demir Tepe, Tahtaköprü (province of Bursa, Turkey). Académie des Sciences, 326, 771-778.

[28] Okay, A.I., 2011. Tavşanlı Zonu: Anatolid-Torid Bloku'nun Dalma-Batmaya Uğramış Kuzey Ucu. MTA Dergisi, 142, 195-226.

[29] Ertürk, D. 2010. Bursa İli Jeotermal Potansiyeli. Süleyman Demirel Üniversitesi, Fen Bilimleri Enstitüsü, Yüksek Lisans Tezi, 94s, Isparta.

[30] Akkaya, G., Kahraman, A., Koray, A., Kaynak, G. 2016. Variation in the radon concentrations and outdoor gamma radiation levels in relation to different geological formations in the thermal regions of Bursa, Turkey. Journal of Radiological Protection, 36(3), 490-503.

[31] Todorovic, N., Nikolov, J., Forkapic, S., Bikit, I., Mrdja, D., Krmar, M., Veskovic, M. 2012. Public Exposure to Radon in Drinking Water in Serbia. Applied Radiation and Isotopes, 70(3), 543-549.

[32] Nikolov, J., Todorovic, N., Forkapic, S., Bikit, I., Mrdja, D. 2011. Radon in Drinking Water in Novi Sad. International Journal of Mathematical, Computational, Physical, Electrical and Computer Engineering, 5(4), 539-542.

[33] National Research Council (NRC), 1999. Risk Assessment of Radon in Drinking Water. Washington: National Academy Press.

[34] Tut Haklıdır, F.S. 2007. Bursa İli ve Çevresindeki Termal, Maden ve Yeraltı Sularının Jeokimyasal İncelenmesi. Dokuz Eylül Üniversitesi, Fen Bilimleri Enstitüsü, Doktora Tezi, 328s, İzmir.

[35] Akkaya, G., Kaynak, G., Kahraman A., Gurler, O. 2012. The Investigation of Radionuclide Distributions in Soil Samples Collected from Bursa, Turkey. Radiation Protection Dosimetry, 152(4), 376-383.

[36] Sakamoto, K., Hamajima, Y., Itoh, K., Yamazaki, K. 1980. Uranium Determinations by Xe-133 in Terrestrial Zircon, Apatite and Chromite-Comparative-Study on Thermal Releases of

Fissiogenic Xeon from Terrestrial and Meteoritic Minerals. Journal of Radioanalytical Chemistry, 60(2), 343-352.

[37] Singh, A.K., Padmasubashini, V., Gopal, L. 2012. Determination of Uranium, Thorium and Rare-earth Elements in Zircon Samples Using ICP-MS. Journal of Radioanalytical Chemistry, 294(1), 19-25.

[38] De Francesco, S., Tommasone, F.P., Cuoco, E., Verrengia, G., Tedescon, D. 2010. Radon Hazard in Shallow Groundwaters: Amplification and Long Term Variability Induced by Rainfall. Science of the Total Environment, 408(4), 779-789.

[39] De Oliveira, J., Mazzilli, B., Sampa, M.H.D.O., Silva, B. 1998. Seasonal Variations of ^{226}Ra and ^{222}Rn in Mineral Spring Waters of Aguas da Prata, Brazil. Applied Radiation and Isotopes, 49(4), 423-427.

[40] Lara, E.G., Rocha, Z., De O. Santos, T., Miguel, R.A., Neto, A.D., De B.C. Menezes, M.A., De Oliveira, A.H. 2011. Distribution of Soil Gas Radon Concentration in the Metropolitan Region of Belo Horizonte, Brazil and Correlations with Litologies and Pedologies. International Nuclear Atlantic Conference, October 24-28, Brazil, 1-10.